Journal of Geodesy manuscript No.
(will be inserted by the editor)

On the influence of the ground track on the gravity field recovery from high-low satellite-to-satellite tracking missions

CHAMP monthly gravity field recovery using the energy balance approach revisited

Matthias Weigelt · Michael G. Sideris · Nico Sneeuw

Received: date / Accepted: date

Abstract In this paper, the influence of the ground track coverage on the quality of a monthly gravity field solution is investigated for the scenario of a high-low satellite-to-satellite tracking mission. Data from the CHAllenging Minisatellite Payload (CHAMP) mission collected in the period April 2002 to February 2004 has been used to recover the gravity field to degree and order 70 on a monthly basis. The quality is primarily restricted by the accuracy of the instruments. Besides, CHAMP passed through a $^{31}/_{2}$ repeat mode three times

M. Weigelt, N. Sneeuw
Institute of Geodesy, Universität Stuttgart
Geschwister-Scholl-Str. 31, 70174 Stuttgart, Germany
Tel.: +49-711-68584637
Fax: +49-711-68583285
E-mail: weigelt@gis.uni-stuttgart.de

M. G. Sideris
Department of Geomatics Engineering, University of Calgary
2500 University Drive N.W., Calgary, AB, T2N 1N4, Canada

during the period of interest resulting in an insufficient spatial sampling and a degraded solution. Contrary to the rule of thumb by *Colombo* (1984), see also *Wagner et al.* (2006), we found that the monthly solutions themselves could be recovered to about degree 30, not 15. In order to improve the monthly gravity solutions, two strategies have been developed: the restriction to a low degree, and the densification of the sampling by the introduction of additional sensitive measurements from contemporaneous satellite missions. The latter method is tested by combining the CHAMP measurements with data form the Gravity Recovery And Climate Experiment (GRACE). Note that the two GRACE satellites are considered independent here, i.e. no use is made of the K-band ranging data. This way, we are able to almost entirely remove the influence of the ground track leaving the accuracy of the instruments as the primary restriction on the quality of a monthly solution. These findings are especially interesting for the upcoming SWARM-mission since it will consist of a similar configuration as the combined CHAMP and GRACE missions.

Keywords CHAMP · aliasing · orthogonality · energy balance approach · variance component estimation

1 Introduction

It is currently accepted that the derivation of time-variable gravity field information from CHAMP-only solutions is not successful. *Reigber et al.* (2005) concluded that monthly gravity solutions solely from CHAMP observations reveal an unrealistic large scattering. *Sneeuw et al.* (2005) tried the recovery using the energy balance approach and kinematic orbits but concluded that the error level of the monthly CHAMP solutions inhibits the revealing of timely variations. Besides the instrument accuracies in general, one of the reasons for the failure to derive time variable gravity is the lack of a consistent set of monthly solutions.

Between months, the spatial data distribution changes due to the slowly decaying orbit. *Colombo* (1984) gave a rule of thumb stating that a spherical harmonic solution of maximum degree L must have at least $\beta > 2L$ revolutions in the time period of interest. Note that it is implicity assumed that the β ground tracks are equally distributed in the spatial domain. A violation of this rule yields a degradation of the solution.

The influence of the ground track on the quality of the gravity field solution attracted first attention for the low-low satellite-to-satellite tracking mission GRACE. It has been investigated by *Yamamoto et al.* (2005) using simulated data and by *Wagner et al.* (2006) using published GRACE solutions. The latter compared the severe loss of accuracy of monthly solutions to degree and order 120 during the $^{61}/_{4}$-resonance orbit in September 2004 to theoretical error estimates from linear perturbation theory, and concluded that the ideal resolution should be only 30x30 confirming Colombo's rule of thumb. Both concluded that the degree RMS degrades by approximately one order of magnitude due to an insufficient sampling. *Klokočník et al.* (2008) extended the investigations of *Wagner et al.* (2006) to the cases of CHAMP and GOCE and predicted future periods of degraded performance of GRACE.

By means of CHAMP, this paper throws additional light on the influence of the ground track on monthly solutions in high-low satellite-to-satellite tracking missions. During the period of interest from April 2002 to February 2004, CHAMP experienced a $^{31}/_{2}$ repeat mode three times resulting in degraded monthly gravity solutions due to a sparse ground track coverage. Presuming a loss of orthogonality in the Legendre polynomials and/or the sine and cosine functions as the primary reason, it is shown by comparison to months with good ground track coverage that the loss of orthogonality is similar for both and thus not responsible for the degradation. Furthermore, a discrepancy to the rule of thumb of *Colombo* (1984) is recognized. According to this, the solution should only be valid to degree and order 15, but a recovery to degree and order 30 is possible. Since the problem is inherent the primary

countermeasure is a change of the orbit configuration (*Klokočník et al.*, 2008). We present two alternative ways of improving the monthly solutions. The first approach is the general restriction to a low degree solution whereas aliasing of high degree signal has to be reduced by using *a priori* gravity field information. The second and more promising approach is the combination with other single satellite missions. Here, the data of the two GRACE satellites are added to the CHAMP data (*Weigelt*, 2007). Note that no use is made of the K-band range-rate measurements and the satellites are considered independent.

Section 2 starts with an overview of the gravity field recovery from CHAMP using the energy balance approach. It is used to derive pseudo-potential observations along the orbit followed by a brute-force spherical harmonic analysis on the sphere (sub-section 2.1). By comparing the monthly solutions of the static gravity field to GGM02S (*Tapley et al.*, 2005), the results can be validated with an independent and more accurate gravity model (sub-section 2.2). This enables the quantification of the influence of the ground track pattern on the gravity solution (sub-section 3.1). Since the degradation of monthly solutions must be reflected in the processing steps, special attention is paid to the loss of orthogonality of the sinusoidal functions in sub-section 3.2. In section 4, the two approaches to counteract the degradation are introduced.

2 Gravity field recovery from CHAMP

2.1 Data processing

The gravity field recovery is separated into three steps: orbit determination; energy balance approach; brute-force spherical harmonic analysis on the sphere. The orbit is derived kinematically, i.e. the positions are estimated in a purely geometrical way. Two years of CHAMP data for the period of April 2002 to February 2004 are provided by the Institute

for Astronomical and Physical Geodesy (IAPG), Technical University Munich (*Švehla and Rothacher*, 2004). The data is considered independent from *a priori* information since no dynamical model is used in their calculation. As only positions are provided, velocities must be derived by numerical differentiation.

The energy balance approach, also called the energy integral approach, is based on the principle of energy conservation (*Jacobi*, 1836; *O'Keefe*, 1957; *Gerlach et al.*, 2003; *Visser et al.*, 2003). The main advantages are its simplicity and the possibility of data processing on desktop computers. The presented equations are given in the Earth-fixed frame. Equivalent expressions for the inertial frame can be found in *Jekeli* (1999). The disturbing potential T along the orbit is calculated by

$$T = \frac{1}{2}\mathbf{v}^T\mathbf{v} - U - Z - \int \left(\mathbf{f} + \sum_i \mathbf{g}_i \right) d\mathbf{x} + c. \tag{1}$$

where $\mathbf{v}$ is the velocity of the satellite. The normal potential U and the centrifugal potential Z can be derived from the position data using standard equations (*Heiskanen and Moritz*, 1967). All known time-variable gravitational accelerations $\mathbf{g}_i$ as well as the non-gravitational accelerations $\mathbf{f}$ are integrated along the orbit $d\mathbf{x}$. The latter are measured using the accelerometer onboard CHAMP. Calibration parameters like bias, drift and scale are determined together with the integration constant c by comparison to potential values along the orbit derived from EGM96 (*Lemoine et al.*, 1998). Although, these parameters could be estimated together with the spherical harmonic coefficients, this preprocessing step is done in order to avoid satellite-specific parameters. Then, the data handling will be easier when combining data of different satellites (sub-section 4.2). All known time-variable gravitational accelerations are derived from models which are summarized in table 1.

[Table 1 about here.]

The last three entries are included in accordance with *Han* (2004) in order to reduce possible temporal aliasing.

Finally, the spherical harmonic analysis with its inherent downward continuation is done using a brute-force least-squares method on the sphere. No regularization is applied for any of the presented results. Further details about the data processing can be found in *Weigelt* (2007).

2.2 Monthly static solutions

Originally, CHAMP was supposed to provide measurements of the global long-wavelength features of the static Earth gravity field and its temporal variations (*Reigber et al.*, 2001). The currently widely accepted procedure to investigate time-variability is based on the derivation of monthly solutions and a long-term mean solution. Their difference is considered as the monthly variation which ideally represents a time-variable gravity signal.

For the investigations here, no mean solution will be subtracted as we are not aiming at the recovery of a time-variable signal. Instead, the static solutions are calculated for every month from April 2002 to February 2004 using a spherical harmonic analysis to degree 70 according to the procedure outlined in sub-section 2.1. Since it is has been shown that no time-variable gravity field can be derived and the measurements are of approximately equal quality, one would expect similar accuracies for each month. In reality, this is not the case; see also *Klokočník et al.* (2008).

[Fig. 1 about here.]

Fig. 1 shows the span of the difference degree RMS of the monthly solutions with respect to GGM02S. The monthly solutions for June 2003 and January 2004 form the boundaries for

the achieved accuracies in the time period of interest, i.e. June 2003 represents the worst and January 2004 the best solution. The discrepancy is approximately one order of magnitude.

[Fig. 2 about here.]

Considering the area-weighted RMS of geoid height differences with respect to GGM02S in the spatial domain, Fig. 2 shows the quality of each monthly solution. Most of them are varying only slightly between 5 cm and 15 cm and a decreasing trend is visible from the beginning to the end of the period which can be connected to the decaying orbit of the satellite. CHAMP loses height from atmospheric drag but the quality of the gravity field solution improves since the satellite is getting closer to the attracting masses. In the three monthly solutions of May 2002, October 2002 and June 2003 however, the RMS-values increase up to 65 cm. The poorer performance cannot be explained by random errors but suggests a systematic effect. Comparing to the orbit height, it is evident that the satellite is at nearly the same height for the three occasions. In sub-section 3.1, we will be able to connect these events to the $^{31}/_{2}$ repeat mode. Since the satellite orbit was raised two times, it passed this mode three times during the period of interest. Note that the monthly solutions have been developed to degree 70 but the calculation of the area-weighted RMS in Fig. 2 is restricted to degree $L = 30$ for an easy comparison with the results in section 4.

3 Aliasing due to the orbit configuration

According to the sampling theorem (*Buttkus*, 1991, §5.2), at least 2 samples are necessary in order to correctly recover one specific frequency of a signal. The maximum resolvable frequency is referred to as *Nyquist frequency* and should be understood as a theoretical boundary. In reality, noise will contaminate the measurements and considerably more samples are necessary in order to recover a signal correctly. If the sampling theorem is violated,

frequencies which are higher than the Nyquist frequency are interpreted as lower frequencies and their energy is projected into the lower part of the spectrum. This effect is referred to as *aliasing* and is often neither reversible nor preventable. It is important to understand aliasing as the result of undersampling which can occur in the spatial sense, as well as in the temporal sense.

In satellite applications, aliasing is mainly caused by:

- the orbit geometry,
- the mixed spectral mapping,
- interactions of the temporal signal and the sampling,
- the negligence of high-degree gravity field signal,
- insufficient background models, e.g. for tidal reductions, and
- incorrect modelling of instrument effects.

The latter three can be summarized as omission errors and are always caused by a deficient mathematical model. They predominantly affect the higher degree terms of a band-limited recovery (*Losch et al.*, 2002; *Sneeuw*, 2000, §6.3).

In sub-section 3.1, the influence of the orbit geometry, which comprises effects related to the orbit height, the sampling density and data gaps within the area of interest, is investigated. The influence of the orbit height on the quality of a gravity solution is twofold. According to Newton's law the signal strength attenuates quadratically with the increasing distance to the attracting body (*Heiskanen and Moritz*, 1967). Its effect has already been observed in Fig. 2. On the other hand, it is also indirectly connected to the ground track pattern and thus to the sampling density. Under the ideal assumption of a sufficiently long time period, a static gravity field and a polar orbit, the Earth could be perfectly covered. The aliasing problem would disappear. Having additionally a uniform data distribution, the

estimation will be unbiased (*Sansò*, 1990). With the limitation to monthly periods and a non-uniform data distribution, the coverage will be imperfect and the estimation biased.

If time-variable signals are present, the satellite senses at the same location two different signals at two different points in time. Whether this time-variable part can be recovered will depend on the time resolution of the satellite mission. Considering monthly solutions as in the case of CHAMP and GRACE, the theoretically shortest resolvable frequency is two-monthly. Any frequencies with shorter periods cannot be recovered, i.e. the temporal spectral bandwidth is restricted to frequencies of two months or longer. Signal outside this spectral bandwidth needs to be modelled and reduced in a preprocessing step in order to avoid aliasing (*Han et al.*, 2003, §5). Typical examples are the corrections due to the half-daily tides or the atmospheric and ocean dealiasing products (*Flechtner*, 2005).

Last but not least, a mixed spectral mapping occurs since the two-dimensional geopotential field is first mapped on a one-dimensional time series along the orbit and subsequently subject to a spherical harmonic analysis, e.g. on a torus or on a sphere. The orthogonality property of the Legendre and sine/cosine function ensures normally a proper decomposition but demands continuous data. Since the measurements are discretized, the orthogonality of the Legendre and sine/cosine function might be lost. In sub-section 3.2, it is investigated if the changing sampling density, which causes the degradation of the gravity solutions in May 2002, October 2002 and June 2003, indeed can be linked to the loss of orthogonality.

3.1 Influence of the ground track

Aiming at the recovery of the gravity field on a monthly basis, the accuracy will be dependent on the data distribution within the month, i.e. on the ground track coverage. Variations

of the ground track coverage are caused by the change of the satellite's mean motion as its height changes.

[Fig. 3 about here.]

[Fig. 4 about here.]

Fig. 3 shows the ground tracks for June 2003 (a month with a sparse ground track coverage) and January 2004 (a month with a particularly good coverage). Comparison with Fig. 2 reveals the connection of the ground track pattern to the quality of a monthly CHAMP solution. Fig. 4 shows the sampling at latitudes of 0° and 80° for a section of 25° around the Greenwich meridian for the two months. It shows that in June 2003, the measurements at the equator are clustered, while in January 2004, the data is spread homogeneously over the equator, and thus higher frequency functions can be fitted. Note that, due to the convergence of the orbit tracks, the sampling at the pole is rather constant, which is the motivation for local calculations in high-latitude areas; see *Garcia* (2002). Consequently, the distribution of the equator crossings governs the maximum resolvable degree.

[Fig. 5 about here.]

Considering the error spectra in the top row of Fig. 5, it becomes obvious that the influence of the ground track is severe. In January 2004, the spectrum is homogeneous whereas in June 2003 the spectrum seems mirrored around the order 31, i.e. signal of cosine coefficients is mapped to sine coefficients and vice-versa. The difference spectra with respect to GGM02S in the bottom row of Fig. 5 show the same pattern, which proves that the effect is real and not just an artifact of the numerical computations. Obviously, some type of aliasing occurs yielding a degraded monthly gravity solution in June 2003.

The relation of the orbit height and the gravity field recovery can be understood if the orbit perturbation spectrum is considered. Since CHAMP is in a near-circular orbit, the sim-

plified perturbation spectrum can be used (*Sneeuw*, 2000):

$$\dot{\psi}_{mk} = k\dot{u} + m\dot{\Lambda} \text{ , with} - L \leq m,k \leq L \text{ ,} \tag{2}$$

where $\dot{\psi}_{mk}$ is the perturbation frequency, L the maximum degree and m the order of the spherical harmonic representation. k is a wavenumber and represents the order in a rotated frame. The drift in the argument of latitude $\dot{u}$ is the sum of the perigee drift $\dot{\omega}$ and the change in the mean anomaly $\dot{M}$. The drift in the longitude of the ascending node $\dot{\Lambda}$ is the sum of the nodal drift $\dot{\Omega}$ and the change in the Greenwich Apparent Sidereal Time $\dot{\Theta}$. For more details and derivations of the simplified perturbation spectrum, the reader is referred to *Kaula* (1966) or *Sneeuw* (2000).

The satellite experiences resonances with the gravity field if the perturbation frequency $\dot{\psi}_{mk}$ becomes equal to zero. Consequently:

$$k\dot{u} = -m\dot{\Lambda} \Rightarrow \frac{k}{m} = \frac{-\dot{\Lambda}}{\dot{u}} = \frac{T_u}{T_\Lambda} = \frac{\alpha}{\beta} \text{ ,} \tag{3}$$

where T_u denotes the orbital revolution period, T_Λ one nodal day, β the number of revolutions and α the number of nodal days. Since k and m are integers and $\frac{k}{m}$ an integer ratio, the ratio $\frac{\beta}{\alpha}$ must also be an integer ratio, i.e. after β revolutions exactly α nodal days have passed. All the ratios need to be relative primes, i.e. they cannot have a common divisor. Furthermore, the smaller the relatives primes are, the sparser will be the ground track. Geometrically, the satellite is in a repeat orbit.

During the months May 2002, October 2002, and June 2003, the satellite is passing through a satellite height of $\approx 400\,\text{km}$ and is experiencing a $^{31}/_{2}$ repeat mode, cf. Fig. 6, i.e. the satellite makes 31 revolutions in 2 nodal days.

[Fig. 6 about here.]

CHAMP passed three times through this mode since it was lifted two times in between. According to the earlier mentioned rule of thumb of *Colombo* (1984), the maximum resolvable degree should be 15, since $\beta = 31$. Looking at Fig. 1, the difference degree RMS curve of June 2003 intersects the signal curve approximately at degree 30 which obviously contradicts this rule. Currently, we cannot offer any explanation or solution to this. We can only state that this discrepancy occurs repeatedly for all three times when the satellite passes the $31/2$ mode and the gravity field can effectively be recovered up to degree and order 30.

Nevertheless, the satellite senses signal beyond this degree and aliasing occurs. It affects the solution primarily in the order (m) direction of the spectrum, which, as equation (2) implies, is the principal parameter for all the geopotential orbit frequencies yielding an appearance that seems mirrored. *Jekeli* (1996) discusses this thoroughly for the case of gridded simulated data and suggests the usage of spherical cap averages as a de-aliasing filter. Here, the data is given along the orbit and interpolation is to be avoided. The development of corresponding filters for irregular sampled data using, e.g. wavelets, is an interesting aspect for future work.

3.2 Orthogonality

In the continuous case, the orthogonality properties of the Legendre and the sine/cosine functions ensure the separation into spherical harmonic coefficients. Since the degradation is visible in the error spectrum of June 2003, it must be reflected in the normal matrix of the least-squares adjustment. It is important to note that we are only interested where the difference between the two months occurs. Due to the non-uniformly distributed and discretized data, a loss of orthogonality is inherent in both months.

Comparing the number of data points per 1°-latitude band in Figs. 7 and 8 on the left panel, January 2004 and June 2003 show virtually no difference.

[Fig. 7 about here.]

[Fig. 8 about here.]

Consequently, the loss of orthogonality of the Legendre polynomials remains unchanged despite the different data distribution. On the other hand, there is a strong modulation of the number of data points per 1° band in the longitudinal direction in June 2003, cf. Fig. 8, bottom panel. Sine and cosine only retain their orthogonality if the data sampling is on an equidistant grid. Since the data sampling in the longitudinal direction depends on the latitude due to the orbit convergence, the orthogonality should be investigated in different latitude bands. Reviewing Fig. 4, the biggest difference is expected where the data density is sparsest, i.e. in the equator area. Note that there is no dependency on the degree since the longitudinal direction is evaluated using $\cos m\lambda$ and $\sin m\lambda$.

The orthogonality properties of the sine and cosine functions have to be evaluated for different cases:

$$\frac{1}{2}(1+\delta_{m,0})\,\delta_{mk} = \frac{1}{2\pi}\int_0^{2\pi}\cos(m\lambda)\cos(k\lambda)\,d\lambda \tag{4a}$$

$$\Rightarrow \frac{1}{2}(1+\delta_{m,0})\,\mathbf{I} \approx \frac{1}{2\pi}\sum_{i=0}^{N}\cos(m\lambda_i)\cos(k\lambda_i)\,\Delta\lambda_i$$

$$= \mathbf{C}^T\mathbf{W}\mathbf{C},$$

$$\frac{1}{2}(1-\delta_{m,0})\,\delta_{mk} = \frac{1}{2\pi}\int_0^{2\pi}\sin(m\lambda)\sin(k\lambda)\,d\lambda \tag{4b}$$

$$\Rightarrow \frac{1}{2}(1-\delta_{m,0})\,\mathbf{I} \approx \frac{1}{2\pi}\sum_{i=0}^{N}\sin(m\lambda_i)\sin(k\lambda_i)\,\Delta\lambda_i$$

$$= \mathbf{S}^T\mathbf{W}\mathbf{S},$$

$$0 = \frac{1}{2\pi}\int_0^{2\pi} \cos(m\lambda)\sin(k\lambda)\,d\lambda \tag{4c}$$

$$\Rightarrow \quad \mathbf{0} \approx \frac{1}{2\pi}\sum_{i=0}^{N} \cos(m\lambda_i)\sin(k\lambda_i)\,\Delta\lambda_i$$

$$= \mathbf{C}^T\mathbf{W}\mathbf{S}$$

where **I** and **0** are the unit and the zero matrix, respectively. **C** and **S** contain the cosine and sine functions for all orders of interest. For the calculations, all measurements within a 1°-band around the equator have been collected and sorted in ascending order. The differences between neighboring samples form the $\Delta\lambda_i$ and are placed on the main diagonal of **W**.

[Fig. 9 about here.]

Fig. 9 shows the orthogonality matrices for January 2004 on the left panel, for June 2003 on the middle panel and their difference on the right panel. The matrices contain in the upper left corner the combination of two cosines, in the upper right and lower left corner a cosine-sine pair, and in the lower right corner the combination of two sine functions. The diagonal elements have been removed according to equations (4a)–(4c) in order to reveal the off-diagonal pattern which is a measure of the loss of orthogonality. Obviously, the data distribution affects both months on different diagonals but the magnitude does not exceed 5%. There is also no specific pattern visible which would enable a connection to the pattern in Fig. 5. Instead, a similar orthogonality is retained in June 2003 and January 2004. Thus, the loss of orthogonality can be excluded as the cause of the degradation of monthly solutions during repeat modes.

4 Improvement strategies

So far, it has been shown that the ground track pattern (and the corresponding orbit configuration) is one of the main culprits of a degenerated global (monthly) gravity field solution.

Since the problem is mostly inherent, it is difficult to overcome. *Klokočník et al.* (2008) mentioned as the primary measure the avoidance of the repeat modes by proper orbit maneuvers. Considering the advanced state of the CHAMP mission, other strategies have to be found in order to improve the monthly solutions.

4.1 Utilization of a priori information

The first possibility is the simple acceptance of the restricted spatial resolution. According to the rule of thumb by *Colombo* (1984), the maximum resolvable degree would be 15 but as mentioned earlier the solution is valid up to degree and order 30, cf. Fig. 1. In the following, the spherical harmonic analysis is done to this degree for all months. Since the satellite is still sensitive to high-degree signal, omitting it would cause aliasing effects for all months as discussed before and thus it needs to be removed beforehand. Since it is assumed that no time-variable signal is present, any recent gravity field model based on CHAMP or GRACE data should yield a reasonable approximation of the high-degree signal. Generally, there is the possibility of low-pass filtering but the conversion of a spectral filter with a passband to degree and order 30 into an along-track filter is not trivial (*Raizner*, 2008).

The high frequency part of the gravity signal is then removed according to

$$T_{L\leq 30} \approx T - T^{apriori}_{L>30}. \tag{5}$$

For the calculations here, a long-term mean solution comprising all the CHAMP data from April 2002 to February 2004 has been used.

[Fig. 10 about here.]

Fig. 10 shows the results of the approach in terms of the spatial RMS of the monthly solutions. Comparing it with Fig. 2, the situation clearly improved for the three months May

2002, October 2002 and June 2003. The RMS reduced from 42.0 cm, 51.0 cm and 62.6 cm, respectively, to 31.0 cm, 33.1 cm and 27.3 cm, but in comparison to the other months a small degradation remains. On the other hand, the situation for the unaffected months worsened surprisingly and the RMS doubled approximately. One possible explanation for this behavior is that the influence of a changed parameter space of the coefficients is visible. Furthermore, the *a priori* field is an approximation of the signal and might cause systematic effects. At the same time, it might be explainable by a reduced ability to handle correlated noise as high-frequency base functions are able to absorb part of this type of noise (*Ditmar and van Eck van der Sluijs*, 2004). In the reduction step, only the deterministic gravity signal has been removed. The noise remains unchanged but has now to be modelled by only $31^2 = 961$ coefficients instead of the former $71^2 = 5041$. Consequently, the lower degree harmonics are more contaminated by noise than before. Possibly, frequency dependent data weighting might be able to improve the solutions, as well (*Ditmar et al.*, 2007).

Although the situation improved for the months with the $31/2$ repeat ground track, it was at the cost of a reduced accuracy in the other months. Another possibility is to improve the sampling by adding information from terrestrial measurements or, more importantly, other satellite missions.

4.2 Combination with GRACE

Ideally, the added measurements should be taken globally in the same period and with similar accuracy as the CHAMP data. The GRACE mission enables exactly this. Note that for this study the K-band measurements are **not** used. Instead, each of the two GRACE satellites is considered as a single satellite mission of the CHAMP-type.

Before looking at the combination, the quality of the monthly static solutions derived from the two GRACE satellites is analyzed. The position data is again provided by the Institute for Astronomical and Physical Geodesy (IAPG), TU Munich, starting from August 2002 with the exception of December 2002 and January 2003. As a consequence, the situation for May 2002 cannot be improved due to data unavailability. The data is processed according to the same procedure outlined in sub-section 2.1.

[Fig. 11 about here.]

Fig. 11 shows, in comparison to CHAMP, the span of the monthly solutions derived from GRACE A and GRACE B in a difference degree-RMS plot with respect to GGM02S. The lower limit is again defined by the minimum difference and the upper limit by the maximum difference. Compared to CHAMP, the solutions of the two GRACE satellites are of similar quality for the very low degrees but show an increasing degradation with increasing degree. The latter can be explained by the downward continuation. Assuming a similar noise level of the instruments onboard the CHAMP and the two GRACE satellites at their corresponding satellite height, the noise is stronger amplified in the case of GRACE due to the downward continuation since the orbital height of the two GRACE satellites was approximately $60-80$ km higher. At the same time, the solutions of GRACE are more consistent since the satellites do not pass a repeat mode during the period of interest.

Clearly, the question of an optimal combination of the data arises. The simplest approach is to combine the data with equal weights, but it implicitly assumes a similar accuracy of all the measurements. Considering that the exact relative accuracy between the measurements of the three satellites is unknown, an equal weighting cannot be assumed optimal. Instead, the weights must be considered unknown and need to be estimated (iteratively) in the adjustment. Variance component estimation offers this possibility.

4.2.1 Variance component estimation

Data in gravity field recovery can be combined on three different levels: observations; normal equations; spherical harmonic coefficients. Variance component estimation (VCE) can handle all three cases. Here, it is used to combine the different data types on the level of normal equations using relative weights between the variance factors σ_i^2 of the data subsets i. Each normal equation/vector of one satellite forms one subset.

The variance factors are unknown random variables since the relative weighting of different data sets is normally unknown. In the VCE, they are derived iteratively in a best invariant quadratic unbiased estimation (BIQUE). The applied methodology follows closely the one outlined in *Koch and Kusche* (2002) except that regularization is not included here and a stochastic trace estimation is not necessary. In each iteration step, the following four steps are done:

1. The unknown parameters $\hat{\mathbf{x}}$ are estimated from a weighted summation of the subsets:

$$\left(\sum_i \omega_i \mathbf{A}_i^T \mathbf{P}_i \mathbf{A}_i\right) \hat{\mathbf{x}} = \sum_i \omega_i \mathbf{A}_i^T \mathbf{P}_i l_i, \tag{6}$$

   where $\mathbf{A}$ is the Jacobian and $\mathbf{P}$ the weighting matrix of a subset i. A relative weighting with respect to the variance of the first subset σ_1^2 using the ratio $\omega_i = \sigma_1^2/\sigma_i^2$ has been introduced. The initial values for σ_i^2 are derived from the monthly static solutions.

2. The contribution of one subset i to the combined solution is denoted as the partial redundancy r_i and calculated as:

$$r_i = n_i - \mathrm{tr}\left(\frac{1}{\sigma_i^2} \mathbf{A}_i^T \mathbf{P}_i \mathbf{A}_i \mathbf{N}^{-1}\right), \tag{7}$$

   where n_i is the number of observation in the subset, "tr" the trace operator and $\mathbf{N}$ the normal matrix of the combined solution.

3. A new variance factor is calculated for each subset:

$$\hat{\sigma}_i^2 = \frac{\hat{\mathbf{v}}_i^T \mathbf{P}_i \hat{\mathbf{v}}_i}{r_i}, \tag{8}$$

   where $\hat{\mathbf{v}}_i$ are the residuals.

4. Set $\sigma_i^2 = \hat{\sigma}_i^2$ and go to 1.

The procedure is repeated until a stopping criterion is fulfilled. For the calculations here, the relative weighting factors ω_i between two steps are considered. If the difference of all elements is smaller than 10^{-3}, the procedure is stopped, which normally takes no more than three to four iterations.

Since subsets can either be formed from the same data source or from different types of data, variance component estimation provides the platform for the combination with terrestrial, airborne, shipborne and altimetry data in the future. Further applications of variance component estimation can be found in *Fotopoulos* (2005) or *van Loon* (2008) for the application to large systems.

4.2.2 Combined monthly static solutions

Since a spherical harmonic analysis has already been performed for each satellite and each month in order to assess the quality of the monthly static fields, the corresponding normal equations can be easily combined. Looking at the range spanned by the best and the worst difference degree RMS with respect to GGM02S of the resulting combined monthly solutions in Fig. 12, it is seen that the combination gives the best of both worlds.

[Fig. 12 about here.]

That is, the GRACE data reduces the span of the CHAMP-only solutions by half an order of magnitude yielding a more consistent set of solutions, and at the same time the

stronger degradation due to the downward continuation in the GRACE-solutions is improved by CHAMP.

[Fig. 13 about here.]

The improved performance is also visible in the spatial difference RMS between the combined solutions and GGM02S in Fig. 13. The months with poor ground track coverage are vastly improved. In October 2002 and June 2003, the RMS dropped from 51.0 cm and 62.6 cm, respectively, to 10.4 cm for both months, which is an improvement by a factor of 5 to 6. The RMS of all other months improved only slightly by approximately 1 cm compared to the CHAMP-only solution. The limiting factor is obviously not the spatial sampling anymore but the overall sensitivity of the instruments.

[Fig. 14 about here.]

For completeness, the relative weights of the GRACE subsets with respect to CHAMP are shown in Fig. 14. Since the measurements of all three satellites are expected to have a similar noise level, a relative weight of 1 is expected. Fig. 14 shows a deviation of ONLY up to 4%. In the beginning the weights of the two GRACE satellites are very similar and indicate a downweighting but in the end of the period, the relative weights of GRACE A and GRACE B start to deviate. A changing noise level for each GPS receiver of the two GRACE satellites is a possible explanation.

5 Conclusions

It has been shown that a sparse ground track coverage has a severe influence on the quality of a gravity field solution. The degradation is visible in the error spectrum as well as in the difference spectrum to independent gravity field models, which suggest that the effect must be

reflected in the normal matrix. Since the latter depends solely on the location of the measurement, its variation can be connected to the geometry of the orbit. However, the insufficient spatial sampling does not cause a loss of orthogonality but results in spatial aliasing since high degree signal is sensed by the satellite which cannot be separated from low degree signal, anymore. The aliasing problem is inherent as long as the orbit remains unchanged. Two possible workarounds are the restriction to a low degree solution or the combination with other data sources. Of the two, the latter outperforms the former and results in an improved performance for months with and without sparse ground track coverage. The combination approach also confirms that spatial aliasing is the cause of the degradation. By adding sufficient additional measurements, the spatial sampling is improved and aliasing is reduced yielding a homogeneous set of monthly gravity solutions.

At the same time, a discrepancy between the rule of thumb by *Colombo* (1984) and the actual recoverable maximum degree has been recognized but cannot be explained currently. According to this rule, the maximum resolvable degree should be 15 during the $^{31}/_{2}$ repeat mode but the solutions are in reality valid to degree and order 30. We currently do not believe that this rule is wrong but it might need refinement for special cases.

Another important outcome of this research is the direct applicability of the combination procedure to the upcoming SWARM mission. The setup of the low flying CHAMP satellite and the two higher GRACE satellites is comparable to this mission.

One possible weakness of our procedure is the energy balance approach itself. It is predominantly an along-track integration of the satellite's velocity, and thus the cross-track and radial information of the gravity field is lost. Other approaches like e.g. the short-arc method (*Mayer-Gürr et al.*, 2005) or the acceleration approach (*Reubelt et al.*, 2003) should outperform the energy integral as they make use of all three components although the latter

approach demands an additional differentiation step. See *Ditmar and van Eck van der Sluijs* (2004) for more details.

Further, the question of an optimal combination is not sufficiently solved. Variance component estimation is just one possible combination approach. In fact, it uses the residuals of the reconstructed signal from the combined model with respect to the measurements. This primarily gives insight into the internal fit of the solution. All comparisons in the spatial and spectral domain, on the other hand, are done with external data, which suggests that the method can be improved by introducing external information. Additionally, only one scalar weighting factor is determined for each subset. The influence of the ground track, on the other hand, is not equal for all coefficients. A degree- and/or order-dependent weighting scheme would be more desirable. Similarly, a frequency dependent data weighting might be an alternative.

In the high-low satellite-to-satellite tracking scenario discussed here, only the static component of the gravity field has been recovered from a time-variable geometry resulting at times in a degraded performance. Obviously, the situation becomes even more complicated for low-low SST data from GRACE as one tries to recover a time-variable gravity field from a time-variable geometry. For a deeper insight, the reader is referred to *Wagner et al.* (2006) and *Klokočník et al.* (2008).

Acknowledgements We like to acknowledge Drazen Švehla from the Institute of Astronomical and Physical Geodesy, TU Munich, for providing the kinematic position data and GFZ Potsdam for providing the acceleration data. Most of the work for this paper was prepared by Matthias Weigelt during his Ph.D. studies at the University of Calgary. Funding for this was provided by the Werner Graupe International Fellowship, the the Department of Geomatics Engineering and the University of Calgary, which is highly appreciated. We also like to thank P. Ditmar and three anonymous reviewers for their useful comments which helped to clarify the content of this paper.

References

Buttkus, B., *Spektralanalyse und Filtertheorie*, Springer, 1991.

Colombo, O., Numerical methods for harmonic analysis on the sphere, *Tech. rep.*, Report No.310, Dept. Geod. Sci. and Surv., Ohio State Univ., Columbus, Ohio, 1983.

Colombo, O., *The global mapping of gravity with two satellites, Publications on Geodesy*, vol. 7 (3), 263 pp., Netherlands Geodetic Commission, Thijsseweg 11, Delft, The Netherlands, 1984.

Ditmar, P., and A. van Eck van der Sluijs, A technique for modeling the Earth's gravity field on the basis of satellite accelerations, *J. Geod.*, *78*, 12–33, 2004.

Ditmar, P., R. Klees, and X. Liu, Frequency-dependent data weighting in global gravity field modeling from satellite data contaminated by non-stationary noise, *J. Geod.*, *81*, 81–96, 2007.

Flechtner, F., AOD1B Product Description Document, *Tech. rep.*, GeoForschungszentrum Potsdam, 2005.

Fotopoulos, G., Calibration of geoid error models via a combined adjustment of ellipsoidal, orthometric and gravimetric geoid height data, *J. Geod.*, *79*, 111 – 123, 2005.

Garcia, R., Local geoid determination from GRACE, Ph.D. thesis, Ohio State University, 2002.

Gerlach, C., N. Sneeuw, P. Visser, and D. Švehla, CHAMP gravity field recovery using the energy balance approach, *Advances in Geosciences*, *1*, 73–80, 2003.

Han, S., Efficient determination of global gravity field from satellite-to-satellite tracking missions, *Celestial Mechanics and Dynamical Astronomy*, *88*, 69–102, 2004.

Han, S., C. Jekeli, and C. Shum, Static and temporal gravity field recovery using GRACE potential difference observables, *Advances in Geosciences*, *1*, 19–26, 2003.

Heiskanen, W., and H. Moritz, *Physical geodesy*, W.H. Freeman and Company San Francisco, 1967.

Jacobi, C., Über ein neues Integral für den Fall der drei Körper, wenn die Bahn des störenden Planeten kreisförmig angenommen und die Masse des gestörten vernachlässigt wird., *Monthly reports of the Berlin Academy*, 1836.

Jekeli, C., Spherical harmonic analysis, aliasing, and filtering, *J. Geod.*, *70*, 214–223, 1996.

Jekeli, C., The determination of gravitational potential differences from satellite-to-satellite tracking, *Celestial Mechanics and Dynamical Astronomy*, *75*, 81–101, 1999.

Kaula, W., *Theory of satellite geodesy*, Blaisdell Publishing Company, 1966.

Klokočník, J., C. Wagner, J. Kostelecký, A. Bezděk, P. Novák, and D. McAdoo, Variations in the accuracy of gravity recovery due to ground track variability: GRACE, CHAMP, and GOCE, *J. Geod.*, *online first*, 2008.

Koch, K., and J. Kusche, Regularization of geopotential determination from satellite data by variance components, *J. Geod.*, *76*, 259–268, 2002.

Lemoine, F., S. Kenyon, J. Factor, R. Trimmer, N. Pavlis, D. Chinn, C. Cox, S. Klosko, S. Luthcke, M. Torrence, Y. Wang, R. Williamson, E. Pavlis, R. Rapp, and T. Olson, The Development of the Joint NASA GSFC and NIMA Geopotential Model EGM96, *Tech. rep.*, NASA Goddard Space Flight Center, Greenbelt, Maryland, 20771 USA, 1998.

Losch, M., B. Sloyan, J. Schröter, and N. Sneeuw, Box inverse models, altimetry and the geoid: Problems with the omission error, *J. Geophy. Res.*, *107*(C7), 15–1 – 15–13, 2002.

Mayer-Gürr, T., K. Ilk, A. Eicker, and M. Feuchtinger, ITG-CHAMP01: a CHAMP gravity field model from short kinematic arcs over a one-year observation period, *J. Geod.*, *78*(7 - 8), 462 – 480, 2005.

O'Keefe, J., An application of jacobi's integral to the motion of an Earth satellite, *The Astronomical Journal*, *62*(8), 266–267, 1957.

Raizner, C., GOCE Data and Gravity Field Model Filter Comparison, Master's thesis, Universität Stuttgart, http://elib.uni-stuttgart.de/opus/volltexte/2008/3403/, 2008.

Reigber, C., H. Lühr, and P. Schwintzer, Announcement of Opportunity for CHAMP, *Tech. rep.*, GFZ Potsdam, 2001.

Reigber, C., R. Schmidt, F. Flechtner, R. König, U. Meyer, K. Neumayer, P. Schwintzer, and S. Zhu, An Earth gravity field model compete to degree and order 150 from GRACE: EIGEN-GRACE02S, *Journal of Geodynamics*, *39*, 1–10, 2005.

Reubelt, T., G. Austen, and E. Grafarend, Harmonic analysis of the Earth's gravitational field by means of semi-conitnuous ephemeris of a low Earth orbiting GPS-tracked satellite. Case study: CHAMP, *J. Geod.*, *77*, 257–278, 2003.

Sansò, F., On the aliasing problem in the spherical harmonic analysis, *J. Geod.*, *64*, 313 – 330, 1990.

Sneeuw, N., Global spherical harmonic analysis by least squares and numerical quadrature methods in historical perspective, *Geophysical Journal International*, *118*, 707 – 716, 1994.

Sneeuw, N., A semi-analytical approach to gravity field analysis from satellite observations, *Reihe C 527*, DGK, 2000.

Sneeuw, N., C. Gerlach, L. Földváry, T. Gruber, T. Peters, R. Rummel, and D. Švehla, One year of time-variable CHAMP-only gravity field models using kinematic orbits, in *A window on the future of geodesy*, *International Association of Geodesy Symposia*, vol. 128, edited by F. Sansò, pp. 288–293, Springer, 2005.

Švehla, D., and M. Rothacher, Kinematic positioning of LEO and GPS satellites and IGS stations on the ground, *Advances in Space Research*, *36*(3), 376 – 381, 2005.

Tapley, B., J. Ries, S. Bettadpur, D. Chambers, M. Cheng, F. Condi, B. Gunter, Z. Kang, P. Nagel, R. Pastor, T. Pekker, S. Poole, and F. Wang, GGM02 - An improved Earth gravity field model from GRACE, *J. Geod.*, *79*, 467 – 478, 2005.

van Loon, J., Functional and stochastic modelling of satellite gravity data, *Tech. Rep. 67*, Netherlands Geodetic Comission - Publications on Geodesy, 2008.

Visser, P., N. Sneeuw, and C. Gerlach, Energy integral method for the gravity field determination from satellite orbit coordinates, *J. Geod.*, *77*, 207–216, 2003.

Wagner, C., D. McAdoo, J. Klokočník, and J. Kostelecký, Degradation of geopotential recovery from short repeat-cycle orbits: application to GRACE monthly fields, *J. Geod.*, *80*(2), 94–103, 2006.

Weigelt, M., Global and local gravity field recovery from satellite-to-satellite tracking, Ph.D. thesis, University of Calgary, http://www.geomatics.ucalgary.ca/graduatetheses, 2007.

Yamamoto, K., T.Otsubo, T. Kubo-oka, and Y. Fukuda, A simulation study of effects of GRACE orbit decay on the gravity field recovery, *Earth Planets Space Letter*, *57*, 291 – 295, 2005.

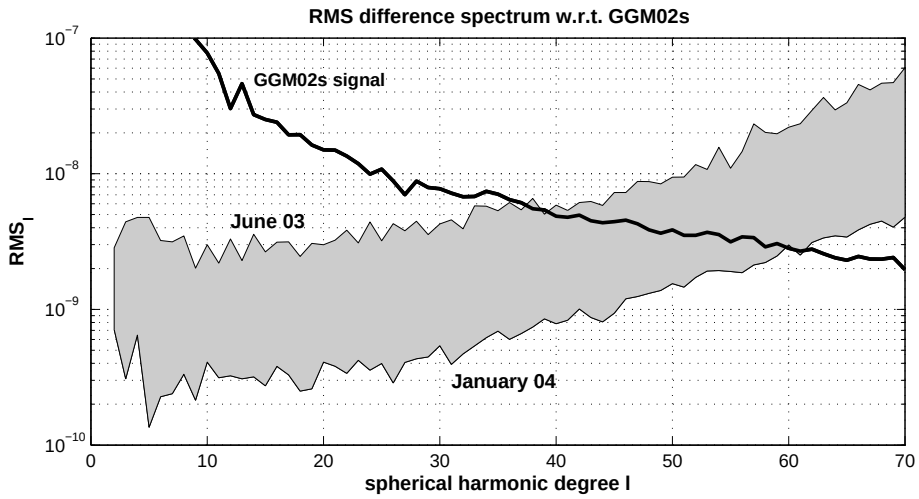

Fig. 1 Span of the difference degree RMS of the monthly static CHAMP solutions with respect to GGM02S. The solution of June 2003 forms the upper boundary representing the worst solution and the one of January 2004 the lower boundary representing the best solution.

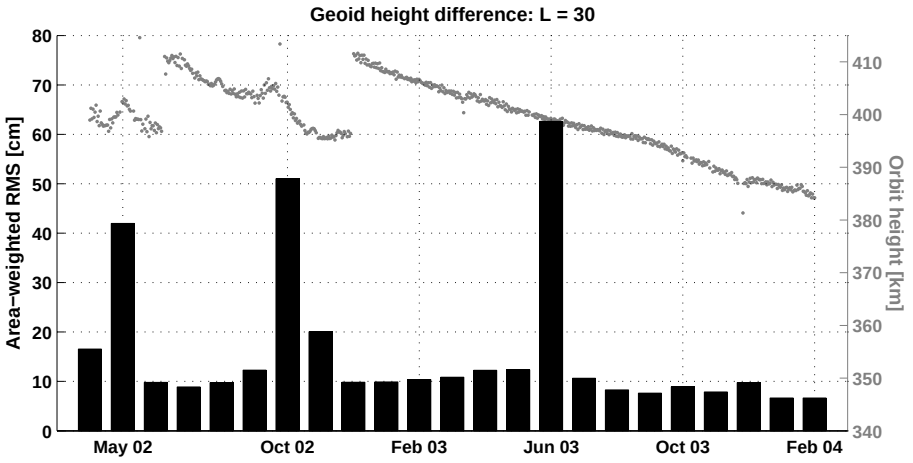

Fig. 2 RMS of the difference between CHAMP monthly solutions and GGM02S in terms of geoid height. In the background and connected to the right y-axis, the orbit height and its daily variation is shown.

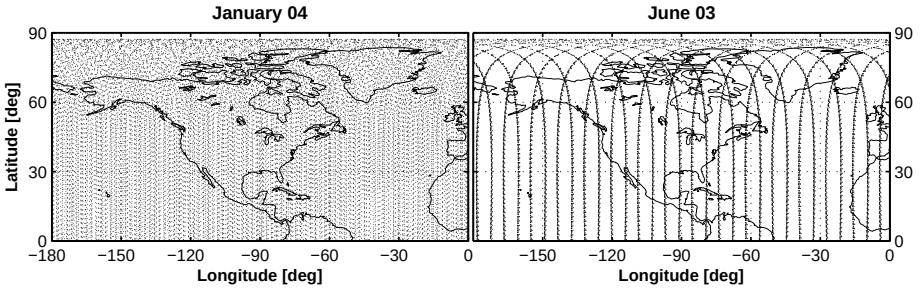

Fig. 3 Ground track coverage over North-America: January 2004 (left) and June 2003 (right)

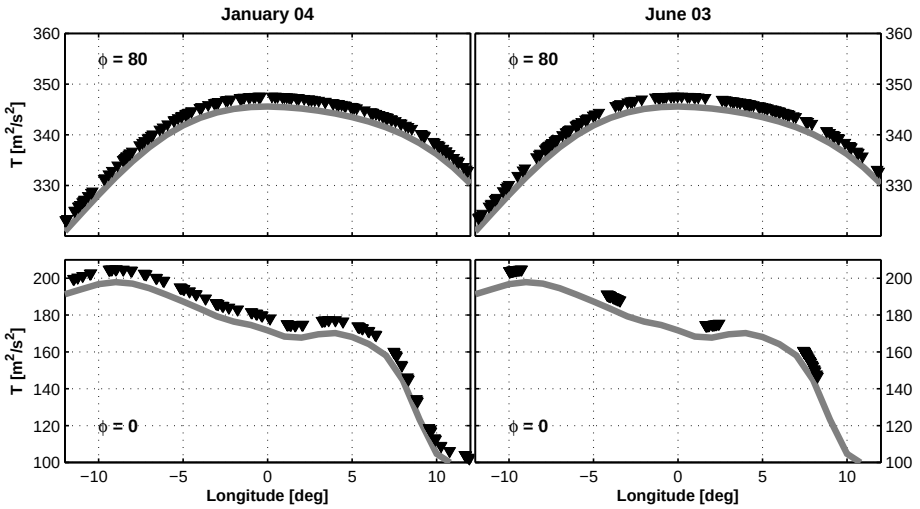

Fig. 4 Sampling (black triangles) of the disturbing potential (solid grey line) for a 25° degree section around the Greenwich meridian: left column for January 2004 and right column for June 2003; top row for a high-latitude parallel ($\phi = 80^\circ$), bottom row for the equator ($\phi = 0^\circ$)

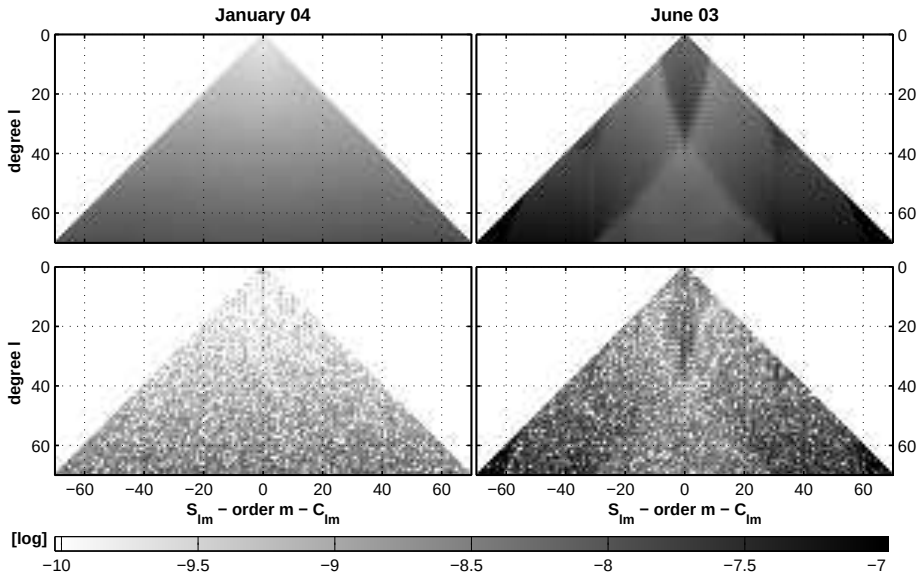

Fig. 5 Error and difference spectra for January 2004 in the left column and for June 2003 in the right column: The top row shows the standard deviations, the bottom row the difference spectra with respect to GGM02S. All figures are on a logarithmic scale.

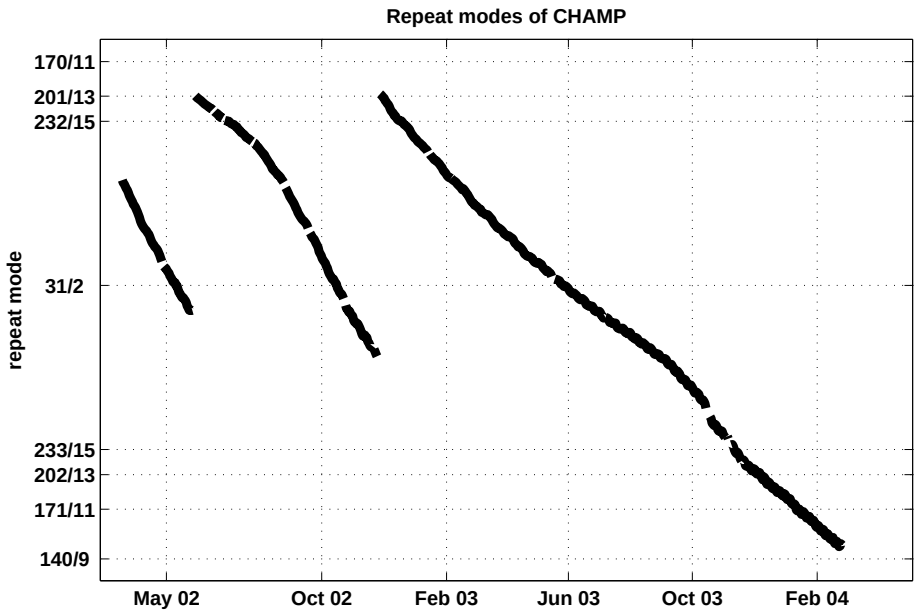

Fig. 6 Repeat modes of the CHAMP satellite

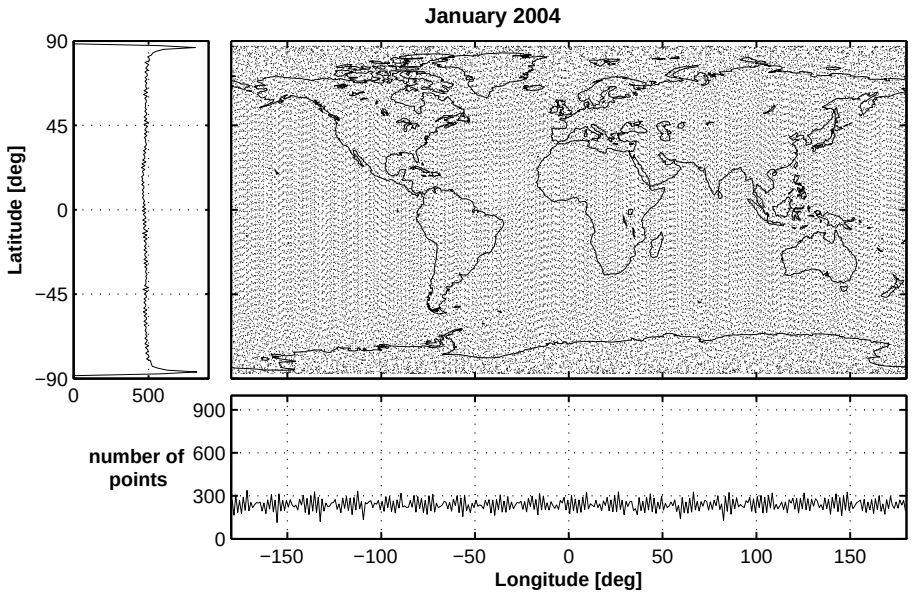

Fig. 7 Ground track and number of points per 1°-band: January 2004

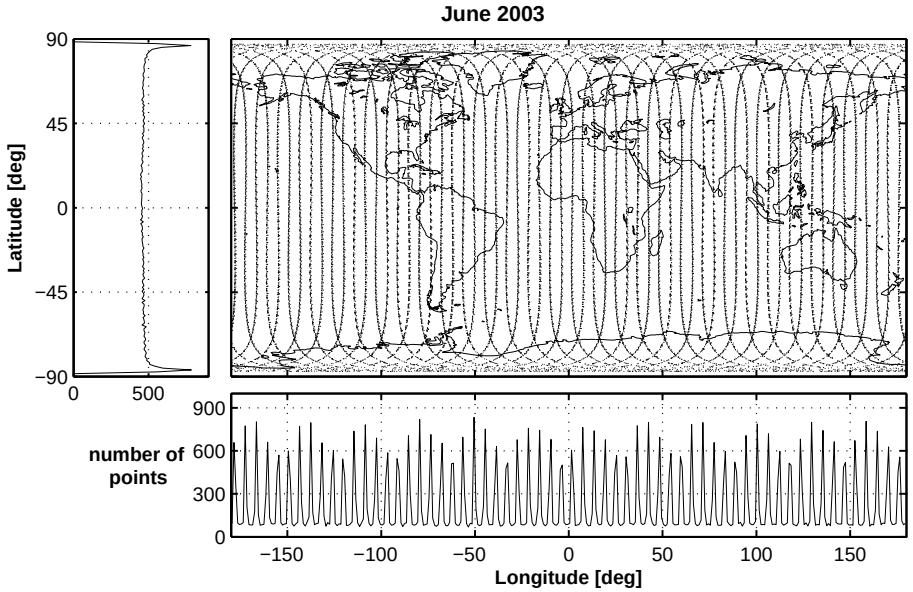

Fig. 8 Ground track and number of points per 1°-band: June 2003

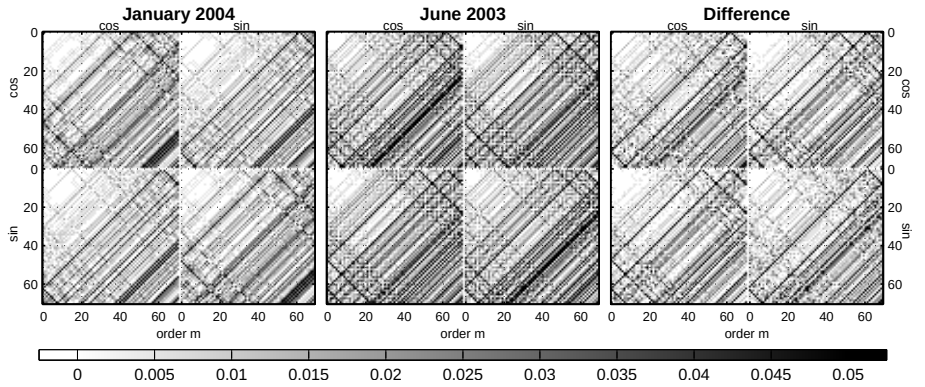

Fig. 9 Sine/cosine orthogonality matrices for an 1°-equatorial band: January 2004 (left panel), June 2003 (middle panel) and their difference on a logarithmic scale (right panel)

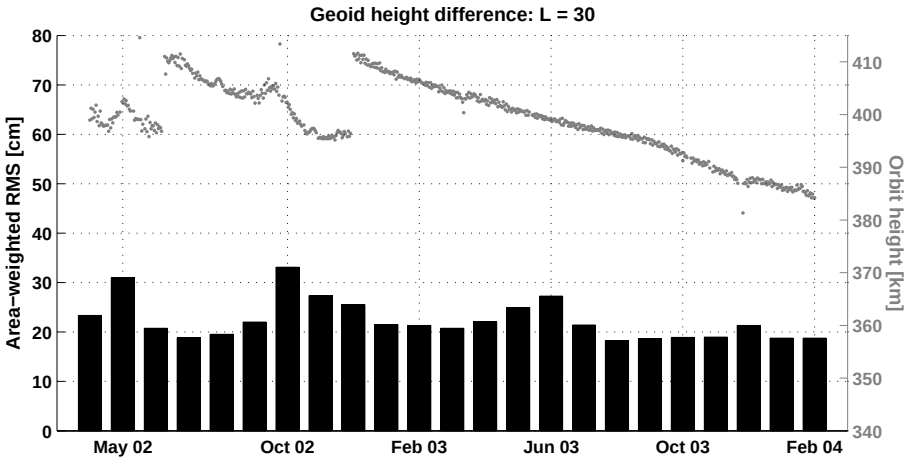

Fig. 10 RMS of the difference between the restricted monthly solutions and GGM02S in terms of geoid height. In the background and connected to the right y-axis, the orbit height and its daily variation is shown.

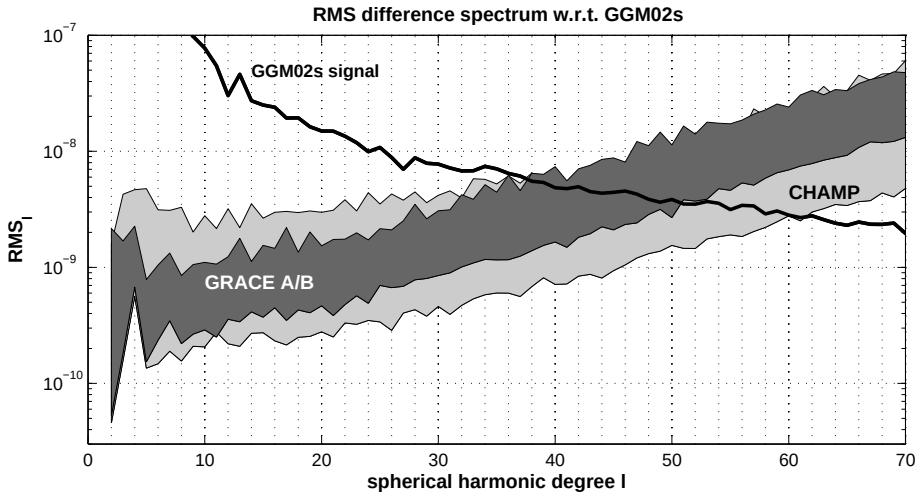

Fig. 11 Span of the difference degree RMS with respect to GGM02S of the monthly static solutions for GRACE (dark gray) and CHAMP (light gray): the worst monthly solution of each data set forms the upper boundary and the best solution the lower boundary.

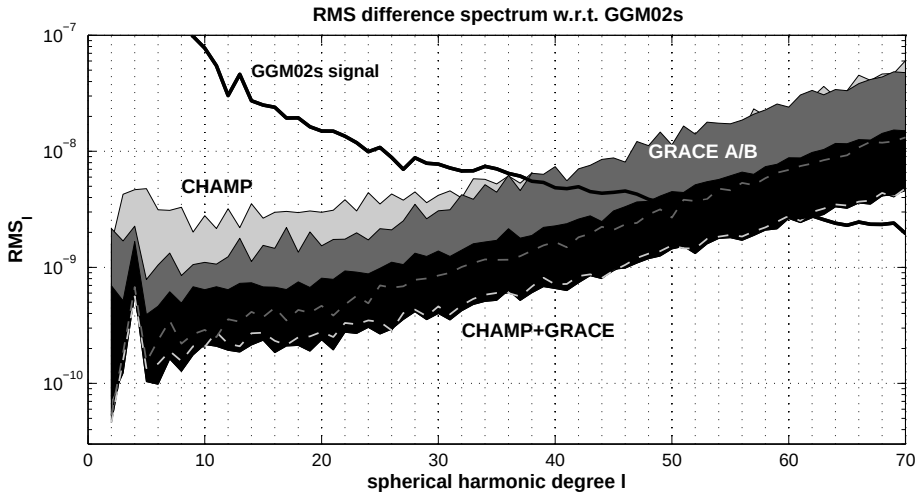

Fig. 12 Span of the difference degree RMS with respect to GGM02S of the monthly static solutions for GRACE (dark gray), CHAMP (light gray) and the combined solution (black): dashed lines indicate the lower boundaries of the CHAMP-only (lower dashed line) and the GRACE solutions (upper dashed line).

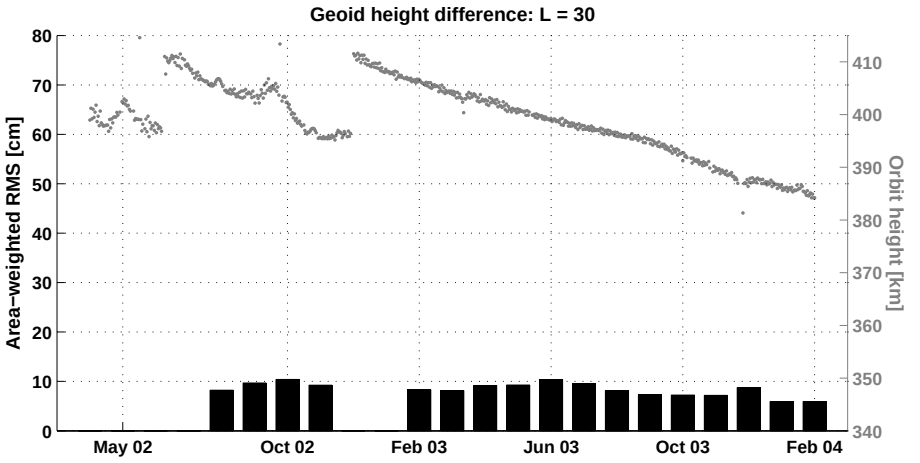

Fig. 13 RMS of the difference between the combined CHAMP/GRACE monthly solutions and GGM02S in terms of geoid height. In the background and connected to the right y-axis, the orbit height of CHAMP and its daily variation is shown.

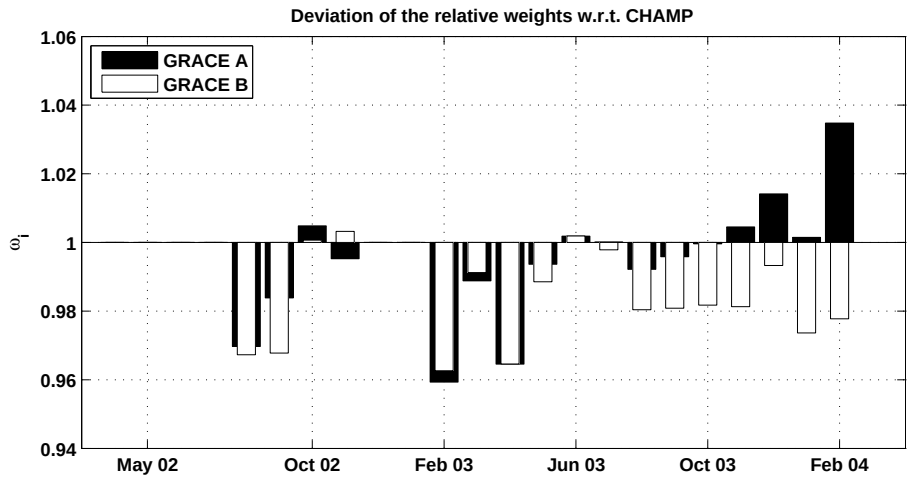

Fig. 14 Relative weights of the GRACE measurements with respect to the CHAMP measurements for each month obtained by the VCE procedure

Table 1 Models utilized for the correction of time-variable effects

source	model
astronomic tide	point masses for Sun and Moon coordinates from DE405
solid Earth tide	IERS Conventions 2003, §6.1
solid Earth pole tide	IERS Conventions 2003, §6.2
ocean tide	FES2004
ocean pole tide	IERS Conventions 2003, §6.3
atmosphere and ocean	AOD1B by GFZ Potsdam
relativistic corrections	IERS Conventions 2003, §10.2